



ORIGINAL ARTICLE

Hepatic kinome atlas: An in-depth identification of kinase pathways in liver fibrosis of humans and rodents

Justin F. Creeden¹  | Zachary A. Kipp² | Mei Xu² | Robert M. Flight^{3,4,5} | Hunter N. B. Moseley^{3,4,5,6,7} | Genesee J. Martinez² | Wang-Hsin Lee² | Khaled Alganem¹ | Ali S. Imami¹ | Megan R. McMullen⁸ | Sanjoy Roychowdhury⁸ | Atta M. Nawabi⁹ | Jennifer A. Hipp¹⁰ | Samir Softic^{2,11} | Steven A. Weinman¹² | Robert McCullumsmith^{1,13} | Laura E. Nagy^{8,14,15} | Terry D. Hinds Jr.^{2,4,16} 

¹Department of Neurosciences, University of Toledo College of Medicine and Life Sciences, Toledo, Ohio, USA

²Department of Pharmacology and Nutritional Sciences, University of Kentucky College of Medicine, Lexington, Kentucky, USA

³Department of Molecular & Cellular Biochemistry, University of Kentucky, Lexington, Kentucky, USA

⁴Markey Cancer Center, University of Kentucky, Lexington, Kentucky, USA

⁵Resource Center for Stable Isotope Resolved Metabolomics, University of Kentucky, Lexington, Kentucky, USA

⁶Institute for Biomedical Informatics, University of Kentucky, Lexington, Kentucky, USA

⁷Center for Clinical and Translational Science, University of Kentucky, Lexington, Kentucky, USA

⁸Department of Inflammation and Immunity, Cleveland Clinic, Cleveland, Ohio, USA

⁹Division of Transplant and Hepatobiliary, Department of Surgery, The University of Kansas Medical Center, Kansas City, Kansas, USA

¹⁰Strata Oncology, Ann Arbor, Michigan, USA

¹¹Department of Pediatrics, University of Kentucky, Lexington, Kentucky, USA

¹²Department of Internal Medicine and Liver Center, University of Kansas Medical Center, Kansas City, Kansas, USA

¹³Neurosciences Institute, ProMedica, Toledo, Ohio, USA

¹⁴Department of Gastroenterology and Hepatology, Center for Liver Disease Research, Cleveland Clinic, Cleveland, Ohio, USA

¹⁵Department of Molecular Medicine, Case Western Reserve University, Cleveland, Ohio, USA

¹⁶Barnstable Brown Diabetes Center, University of Kentucky College of Medicine, Lexington, Kentucky, USA

Correspondence

Terry D. Hinds, Jr., Department of Pharmacology and Nutritional Sciences, University of Kentucky College of Medicine, 760 Press Ave., Healthy Kentucky Research Building (HKRB) 221, Lexington, KY 40508, USA.
Email: Terry.Hinds@uky.edu

Funding information

Supported by the National Institutes of Health (1R01DK121797, NIMH R01 MH107487, R01 AG057598, R01 MH121102, P50 AA024333); the University of Toledo Foundation; National Science New Network Foundation (2020026); the Biostatistics and

Abstract

Background and Aims: Resolution of pathways that converge to induce deleterious effects in hepatic diseases, such as in the later stages, have potential antifibrotic effects that may improve outcomes. We aimed to explore whether humans and rodents display similar fibrotic signaling networks.

Approach and Results: We assiduously mapped kinase pathways using 340 substrate targets, upstream bioinformatic analysis of kinase pathways, and over 2000 random sampling iterations using the PamGene PamStation kinome microarray chip technology. Using this technology, we characterized

Abbreviations: CD, choline-deficient; DDR1, discoidin domain receptor tyrosine kinase 1; DM1, dystrophy type 1; DMPK, DM1 protein kinase; ECM, extracellular matrix; HFD+F, high-fat diet plus fructose; INSR, insulin receptor; KEGG, Kyoto Encyclopedia of Genes and Genomes; MAFLD, metabolic-associated fatty liver disease; MAPK, mitogen-activated protein kinase; pDDR1, phosphorylation of DDR1; PI3K, phosphatidylinositol-3-kinase; pINSR, phosphorylation of INSR; PK, protein kinase; PTK, protein tyrosine kinase; STK, serine/threonine kinase; TK, tyrosine kinase; α SMA, α -smooth muscle actin.

This is an open access article under the terms of the [Creative Commons Attribution-NonCommercial-NoDerivs](https://creativecommons.org/licenses/by-nc-nd/4.0/) License, which permits use and distribution in any medium, provided the original work is properly cited, the use is non-commercial and no modifications or adaptations are made.

© 2022 The Authors. *Hepatology* published by Wiley Periodicals LLC on behalf of American Association for the Study of Liver Diseases.

Bioinformatics Shared Resource Facility of the University of Kentucky Markey Cancer Center (P30CA177558); and by the University of Kentucky Office of the Vice President for Research through the Diabetes and Obesity Research Priority Area

a large number of kinases with altered activity in liver fibrosis of both species. Gene expression and immunostaining analyses validated many of these kinases as *bona fide* signaling events. Surprisingly, the insulin receptor emerged as a considerable protein tyrosine kinase that is hyperactive in fibrotic liver disease in humans and rodents. Discoidin domain receptor tyrosine kinase, activated by collagen that increases during fibrosis, was another hyperactive protein tyrosine kinase in humans and rodents with fibrosis. The serine/threonine kinases found to be the most active in fibrosis were dystrophy type 1 protein kinase and members of the protein kinase family of kinases. We compared the fibrotic events over four models: humans with cirrhosis and three murine models with differing levels of fibrosis, including two models of fatty liver disease with emerging fibrosis. The data demonstrate a high concordance between human and rodent hepatic kinome signaling that focalizes, as shown by our network analysis of detrimental pathways.

Conclusions: Our findings establish a comprehensive kinase atlas for liver fibrosis, which identifies analogous signaling events conserved among humans and rodents.

INTRODUCTION

Liver fibrosis serves as a critical prognostic indicator and correlative of severe hepatic disease,^[1] which drives death and morbidity.^[2] The proliferating fibrotic network that occurs during liver dysfunction happens from the activation of HSC proliferation, which sheds their extracellular matrix (ECM) components that eventually cause the liver to harden.^[3] If left unchecked, the accumulation of ECM components facilitates liver disease progression to hepatic cirrhosis and life-threatening liver failure.^[4] It is currently thought that liver fibrosis is a deleterious event that is irreversible. However, our current knowledge of the in-depth signaling mechanisms that encourage these insults is limited.

Numerous factors activate hepatic fibrosis, one being damage to the liver. The normal healing procedure commences with an integrated network of protein kinases (PKs) that drives “repair” of the wounded liver.^[4] The accumulation of fat in the liver (simple steatosis) may be a precursor that can initiate hepatic fibrosis.^[4] Long-term high-fat diets or genetic factors can cause fat accumulation in the liver to the level that leads to the metabolic-associated fatty liver disease (MAFLD) that induces hepatic insulin resistance and type 2 diabetes.^[5–11] MAFLD can progress to NASH, which also consists of hepatic fibrosis and inflammation.^[12] For this reason, the treatment of MAFLD with insulin sensitizers is thought to be a preventive measure that protects hepatocytes. If untreated, signals in NASH eventually induce hepatocyte death and activate HSCs that cause a rearrangement of liver cells

that can worsen and progress to cirrhosis.^[12] Other injurious events induce fibrosis without fat accumulation by activating HSC proliferation, such as carbon tetrachloride (CCl₄).^[13] CCl₄ drives HSCs to proliferate and activates genes for collagen and ECM that commence fibrotic episodes.^[14]

There is an imbalance in signaling mechanisms in fibrosis and cirrhosis for the liver cell types, in which hepatocytes are dying (necrosis and apoptosis) and stellate cells are actively growing and shedding ECM. PKs regulate the activity of target proteins through the transference of phosphate groups, which often leads to downstream signaling that induces gene activation and epigenetic changes.^[3,4] These circumstances can lead to whole-genome and physiological changes that might be permanent, such as making the disease irreversible, which is present in patients with cirrhosis with severe fibrosis, and the buildup of collagen in the liver that causes scarring. Increased knowledge of the molecular pathways involved in the progression of hepatic fibrosis is needed, which might open therapeutic targets for reversing liver damage.

Although numerous studies on pathways show signaling mechanisms, no studies have analyzed these events concomitantly. The comprehensive pathways and their interconnectivity that might control these inverse situations are mostly unknown. This study leveraged the PamGene kinome technology with multiple bioinformatic pipelines and validation studies to identify altered kinase pathways. Our strategy was to comprehensively map the active kinome of hepatic fibrosis in humans and rodents and determine whether they had

similar signaling mechanisms. We meticulously performed high-throughput kinomic activity assays capable of simultaneously quantifying the enzymatic activity corresponding to over 350 unique kinases, covering most of the kinome. We show that the overactive signaling pathways in humans with fibrosis were also conserved and primarily changed in mice. Interestingly, we found that the insulin receptor (INSR) and discoidin domain receptor tyrosine kinase 1 (DDR1) were the primary tyrosine kinases, and dystrophy type 1 (DM1) protein kinase (DMPK) and the PK family (PKA, PKB/AKT, PKC, and PKG) were the major serine/threonine kinases that contributed to fibrosis, and these were analogous in humans and rodents. In the kinome atlas presented here, we show the most extensively combined map of kinase families and subfamilies that have been currently assembled, which provides a conglomeration of signaling pathways that are hyper-active and hypo-active in fibrosis.

METHODS

Human subjects

All studies using human samples were approved by the Human Subjects Committee of the University of Kansas Medical Center.

Animal experimentation

All animal procedures were approved by the Cleveland Clinic Institutional Animal Care and Use Committee (IACUC) for the CCl₄ administration to mice and mouse feeding with choline-deficient L-amino acid–defined diet. The mouse fed with high fat supplemented with fructose diet were approved by the IACUC committee at the University of Kentucky.

Statistical and correlation analyses

The kinome array and upstream kinase identification, interaction network analysis, pathway and annotation enrichment analysis, and correlation analysis are described further in the [Supporting Methods](#). The Student's *t* tests were performed on quantitative real-time PCR data to detect statistical differences between control and liver fibrosis groups, with *p* values adjusted for multiple testing corrections within each human and mouse using the Benjamini-Hochberg method.^[15] Adjusted *p* alpha (false discovery rate) ≤ 0.05 was considered statistically significant.

All of the procedures, methods, and analysis are described in more detail in the [Supporting Methods](#).

RESULTS

Interrogation of kinase pathways in humans and mice with fibrosis

To identify kinases that might drive fibrotic pathways among humans and rodents, we quantified the activity of 196 tyrosine (protein tyrosine kinase [PTK]) peptide substrates and 144 serine/threonine kinase (STK) peptide substrates in liver samples from humans with fibrosis/cirrhosis or healthy control and livers from rodents with fibrosis or healthy control. To visually represent the kinase activity demonstrated in the phosphorylation level of these 340 kinase peptide substrates that were changed with fibrosis relative to their healthy control, and an upstream analysis performed with the data deconvoluted into a kinase tree for humans ([Figure 1A](#)) and mice ([Figure 1B](#)). The higher mean final kinase scores determine a more substantial role in the observed phosphorylation changes between fibrosis and normal control samples. Mean final scores for all identified PTK and STK kinases were mapped according to paralogy. The kinase activity results were charted as bubble plots with node size based on *Z* scores in red (highest changed *Z*, mean node = 4), pink (mean node = 2), or gray (mean node = 1) circles to visually indicate potential clusters of kinase families that are changed with fibrosis in humans or rodents. The kinase tree data show significant clusters for the tyrosine kinase (TK) and the serine/threonine AGC kinase families. There was also some clustering in the CAMK and CMGC kinase families but to a lesser extent. The Tyrosine Kinase-Like, STE, Cell Kinase 1, and atypical kinase families were primarily unchanged, but some specific targets in these families were changed. Next, we systematically analyze each kinase family and subfamilies to determine which pathways change most in humans and rodents with fibrosis.

Concordance between human and mouse data

Shapiro-Wilk normality tests and quantile-quantile plots indicate that the kinase activity data sets are not normally distributed (human kinase family data: $W = 0.84641$, p value = 8.825×10^{-6} , rodent kinase family data: $W = 0.82763$, p value = 2.822×10^{-6} , human individual kinase data: $W = 0.82247$, p value = 1.585×10^{-12} , mouse kinase family data: $W = 0.79478$, p value = 1.446×10^{-13}). [Figure 2A,B](#) shows a sample-sample correlation heatmap of log-transformed peptide phosphorylation data from both human and mouse analytical replicates. This correlation matrix analysis shows human and mouse fibrosis groups clustering closer together (0.89 median Information-Content-Informed Kendall-tau Correlation

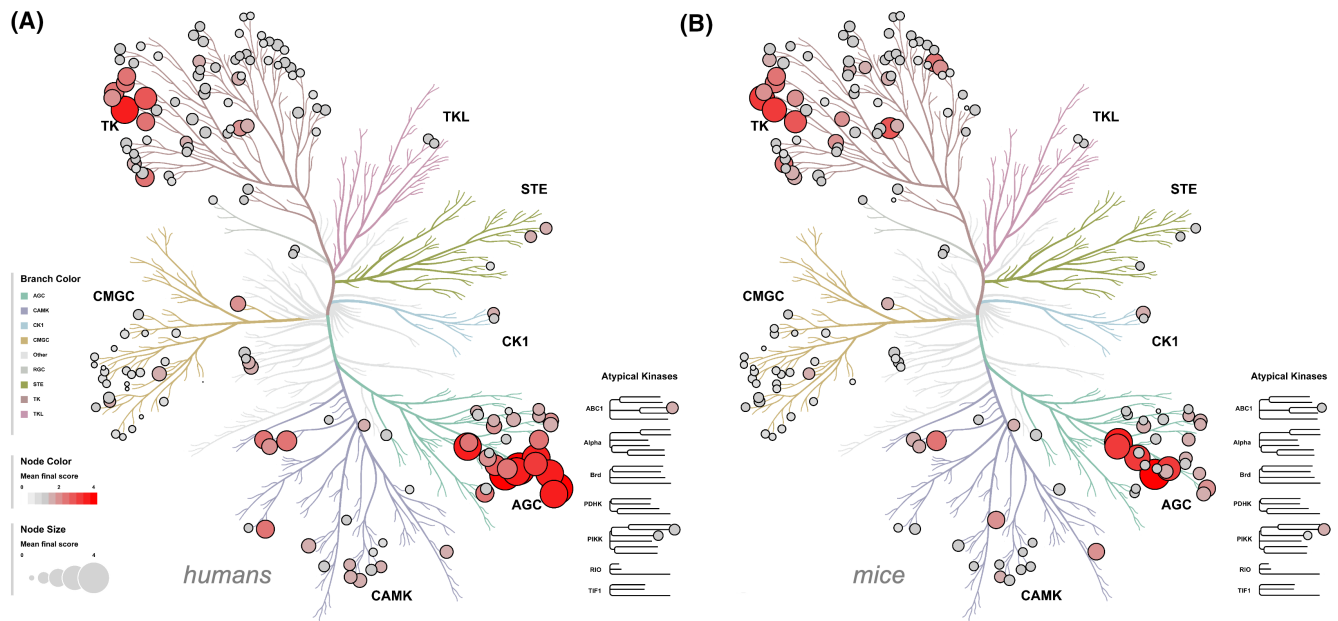


FIGURE 1 Paralogous phylogenetic relationships between differentially altered kinases in humans and rodents. (A) Human liver fibrosis compared with normal control samples. (B) mouse fibrosis compared with normal control samples. Node color and size are the mean final kinase score that corresponds to the bubble plot on the paralogous phylogenetic trees. Abbreviations: TK, tyrosine kinase; TKL, Tyrosine Kinase-Like.

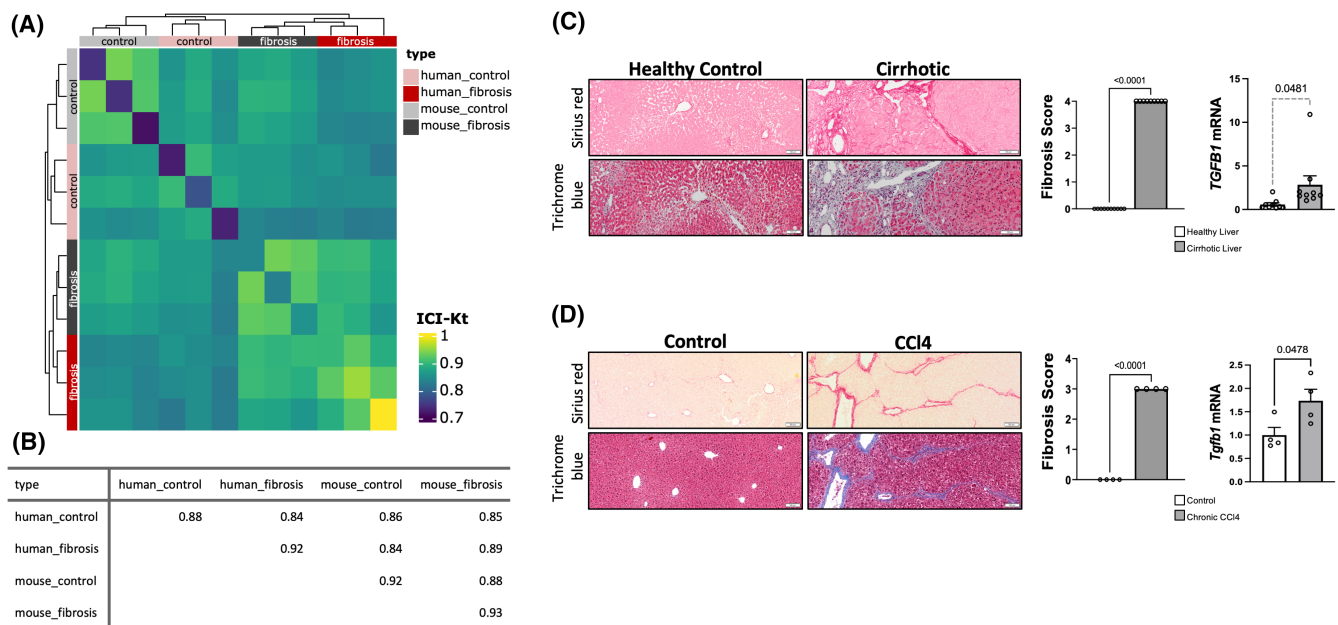


FIGURE 2 Data concordance heatmap. (A) Sample-sample correlation heatmap of analytical replicate samples from aggregate human and mouse control and fibrotic liver samples. Diagonal entries represent the percentage of non-missing values in each analytical sample. Correlations were calculated using Information-Content-Informed Kendall-tau Correlation (ICI-Kt) (available online: <https://github.com/MoseleyBioinformaticsLab/ICKendallTau>) using features that had nonzero values in at least one sample. Feature values < 30 were treated as missing. (B) Median ICI-Kt correlations among samples within a type (diagonal) and between types (off-diagonal). (C,D) Sirius red and trichrome blue staining (scale bar = 100 μ m) in the livers from human cirrhotic and healthy control and chronic CCl₄ and vehicle control-treated mice, fibrosis score, and TGF-B1 or Tgf-b1 mRNA expression

[ICI-kt]) than either of the two humans (0.84 median ICI-Kt control vs. fibrosis) or mouse groups (0.88 median ICI-Kt correlation control vs. fibrosis), demonstrating the high similarity between human and mouse liver elevated fibrosis kinase activity. Furthermore,

all sample-sample correlations have a p value < 2.2×10^{-16} (i.e., below the machine precision limit).

Next, to visually compare and quantitate the level of fibrosis in the human and mouse livers, we did sirius red and trichrome blue staining of the human cirrhotic

and healthy livers and the murine livers treated with chronic CCl_4 or vehicle control. The results show that the healthy control human and vehicle control mouse livers had no fibrosis present and that cirrhotic human and chronic CCl_4 -treated mice had severe fibrosis to the level of a fibrosis score of 4.0 and 3.0, respectively (Figure 2C,D). Also, in comparison, both the human and murine livers with fibrosis had significantly higher TGF- β mRNA expression, which is an established marker of fibrosis.^[16] These data indicate a closely related data concordance between human and murine fibrosis that has visual similarities among these models.

Therefore, we performed separate pathway and annotation enrichment analyses using the human and mouse differential kinase activity, respectively (Table S7). The ICI-Kt correlation between human and mouse enrichment-adjusted p values for Kyoto Encyclopedia of Genes and Genomes (KEGG) pathways, REACTOME pathways, and Gene Ontology Biological Process annotations are 0.73 ($p = 3.9 \times 10^{-24}$), 0.62 ($p = 7.7 \times 10^{-26}$), and 0.78 ($p = 4.3 \times 10^{-165}$), respectively (see Supporting Information for correlation plots in Figure 1 and full pathway enrichment tables in Table S6). This clearly shows that fibrotic versus control differential kinase activity in humans and mice is very similar at the pathway and

biological process level. Moreover, the three most enriched KEGG pathways are the phosphatidylinositol-3-kinase (PI3K)–Akt signaling pathway (human-adjusted p value = 5.9×10^{-17}), Ras signaling pathway (human-adjusted p value = 2.5×10^{-14}), and EGF receptor tyrosine kinase inhibitor resistance pathway (human-adjusted p value = 2.3×10^{-14}). All three of these pathways have known associations with liver fibrosis.^[17,18]

Tyrosine kinase families changed with fibrosis

To determine TK families that might change with fibrosis, we compiled data from substrate phosphorylation events from the PamGene analysis into heatmaps (Figure 3A,B). We used bioinformatic analyses (described in Upstream Kinase Identification) from these data to identify upstream kinases responsible for the observed differential phosphorylation patterns of peptide substrates (Table S3). An aggregation of the data according to the TK family waterfall plot showed that *DDR1* and *INSR* were the most differential active kinases (Figure 3C,D). We next compared the observed number of differentially phosphorylated peptide substrates

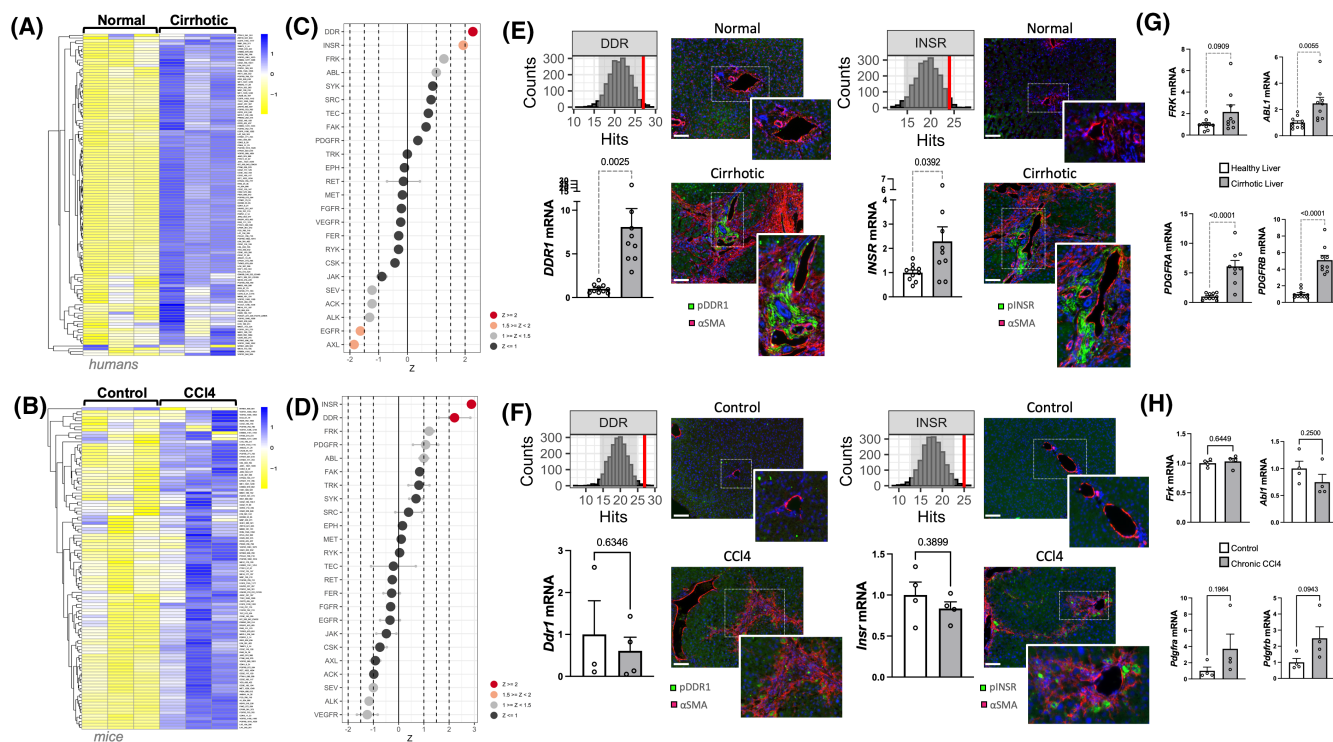


FIGURE 3 Identification of tyrosine kinase families changed in fibrosis of humans and rodents. Heatmap of substrate phosphorylation levels for tyrosine kinases and waterfall plot of tyrosine family of kinases in humans (A) and mice (B) for fibrotic samples compared with their control. Upstream tyrosine kinase families were identified by peptide substrate phosphorylation in human (C), mice fibrotic (D), and normal samples. Quantification of discoidin domain receptor (DDR) and insulin receptor (INSR; $Z > 2$) by histogram peacock plots, mRNA expression measured via real-time PCR, and immunostaining with antibodies for phospho-DDR1 (pDDR1), phospho-INSR (pINSR), or α -smooth muscle actin (α SMA) (scale bar = 50 μm) in humans (E) and mice (F) for fibrotic samples compared with their control. Real-time PCR measurement of mRNA expression of midlevel differentially changed ($Z = 2$ –1.5) tyrosine kinases in humans (G) and mice (H)

targeted by each kinase or kinase family against 2000 random sampling iterations, selecting the same number of peptide substrates from the pool of 196 (PTK) or 144 (STK) (depending on whether TK or STK are being measured) peptide substrates found on the arrays. The number of experimentally determined differentially phosphorylated peptide substrates targeted by a given kinase or kinase family in relation to the number of randomly selected peptide substrates targeted by that same kinase or kinase family in each of the thousands of random sampling events indicates the significance of the kinase or kinase family of interest to the differential phosphorylation patterns observed between fibrosis and normal samples. These data are represented here as annotated histograms, herein referred to as peacock plots. The peacock plots for the DDR and INSR kinase families indicate significantly differential kinase activity in humans (Figure 3E) and rodents (Figure 3F). To determine whether DDR1 and INSR were changed at the gene level, we measured mRNA by real-time PCR and compared this with the peacock plot of the substrate analysis. The mRNA expression was significantly increased for *DDR1* ($p = 0.0025$) and *INSR* ($p = 0.0392$) in humans with cirrhosis/fibrosis (Figure 3E), but no statistically significant difference was detected in the mouse model of fibrosis (Figure 3F). The peacock plots indicate differential signaling of DDR and INSR kinase family activity on their substrates, which is represented by the number of kinase family peptide targets (x-axis; hits) experimentally identified as differentially phosphorylated in fibrosis (red line) or identified during thousands of random sampling events (gray bars). The number of instances in which a given number of kinases or the family of peptide targets were selected from 2000 random sampling iterations is represented by the height of each gray bar (y-axis; count).

To validate the level of phosphorylation of DDR1 (pDDR1) and INSR (pINSR) and to determine whether they are enhanced in a specific liver-cell type, we performed immunostaining using antibodies that are phosphorylation-specific and for α -smooth muscle actin (α SMA), a marker indicating hepatic stellate cells as previously identified.^[19] The pDDR1 and pINSR had low immunostaining in normal healthy human livers and vehicle-treated mice livers, but the staining was much more pronounced in the human cirrhotic livers and mice with chronic CCl₄ treatment (Figure 3E,F). The pDDR1 and pINSR immunostaining were colocalized with the α SMA in human cirrhotic livers and the chronic CCl₄ treatment mice livers, indicating that this might be an effect that is specific to HSCs.

These data are presented above mRNA measures, demonstrating differential gene-expression levels between human fibrosis samples and normal human samples, or fibrosis rodent samples and normal rodent samples. The TK families that were partly altered, as indicated by light gray circles, were fyn related Src

family tyrosine kinase (FRK), ABL, and Platelet-derived growth factor receptor. We therefore measured the mRNA levels of these genes to determine whether they were also changed. The *PDGFRA*, *PDGFRB*, and *ABL1* were all higher in humans with fibrosis at a statistically significant level (adjusted p value < 0.018), but not *FRK* (adjusted p value = 0.124) or any of these genes measured in the mouse model of fibrosis (Figure 3G,H).

To further interrogate the TK group, we analyzed individual kinases consisting of the TK tree branches that were identified as significantly changed among kinases in humans and rodents (Figure 4A,B). As indicated by the upstream analysis shown by the waterfall plots in Figure 4C,D, considerable changes were observed for the Src family kinases (LCK, FYN, SRC, YES1, BLK, LYN, and HCK), Abl family (ABL1), Syk family (SYK), and Met family (RON/macrophage stimulating 1 receptor). To delve further into this evaluation, we performed random sampling analyses and quantification of gene-expression changes for the kinases conserved among the two species. The peacock plots above each mRNA show the observed number of differentially phosphorylated peptide substrates (indicated by the red line) compared with thousands of iterations of random peptide selection (Figure 4E,F). The data for humans with fibrosis indicate that all TK assignments are not the result of chance, as indicated by the red line to the right, except one kinase, RON. These patterns were mostly conserved between humans and rodents. The human gene expression data for these targets showed altered Src family kinases (FYN, SRC, BLK, and HCK), ABL1, and SYK, which were all higher compared with human fibrosis. The analysis in mice showed that these kinases were also hyperactive, but no significant changes in gene expression were observed (Figure 4F).

Assimilation of STK families that are altered with fibrosis

The STK signaling events typically occur after a TK signaling event has been sent or by intracellular mechanisms that activate signaling mechanisms. We interrogated the STKs that might be hyperactive or hypo-active in fibrosis. We organized the results of the substrate phosphorylation events in heatmaps to show how STK signaling events differ among humans (Figure 5A) and mice (Figure 5B) with fibrosis. Next, we compared the most differentially altered kinases in a waterfall plot based on the Z score for STKs that changed with fibrosis (Figure 5C,D). The highest families of STK events changed in our analysis were DMPK, PKA, and PKG. The peacock plots for DMPK and protein kinase cyclic adenosine monophosphate (cAMP)-activated catalytic subunit alpha (*PRKACA/PKA α*) in humans showed that their kinase activity was higher in humans and mice (Figure 5E,F). The mRNA expression levels

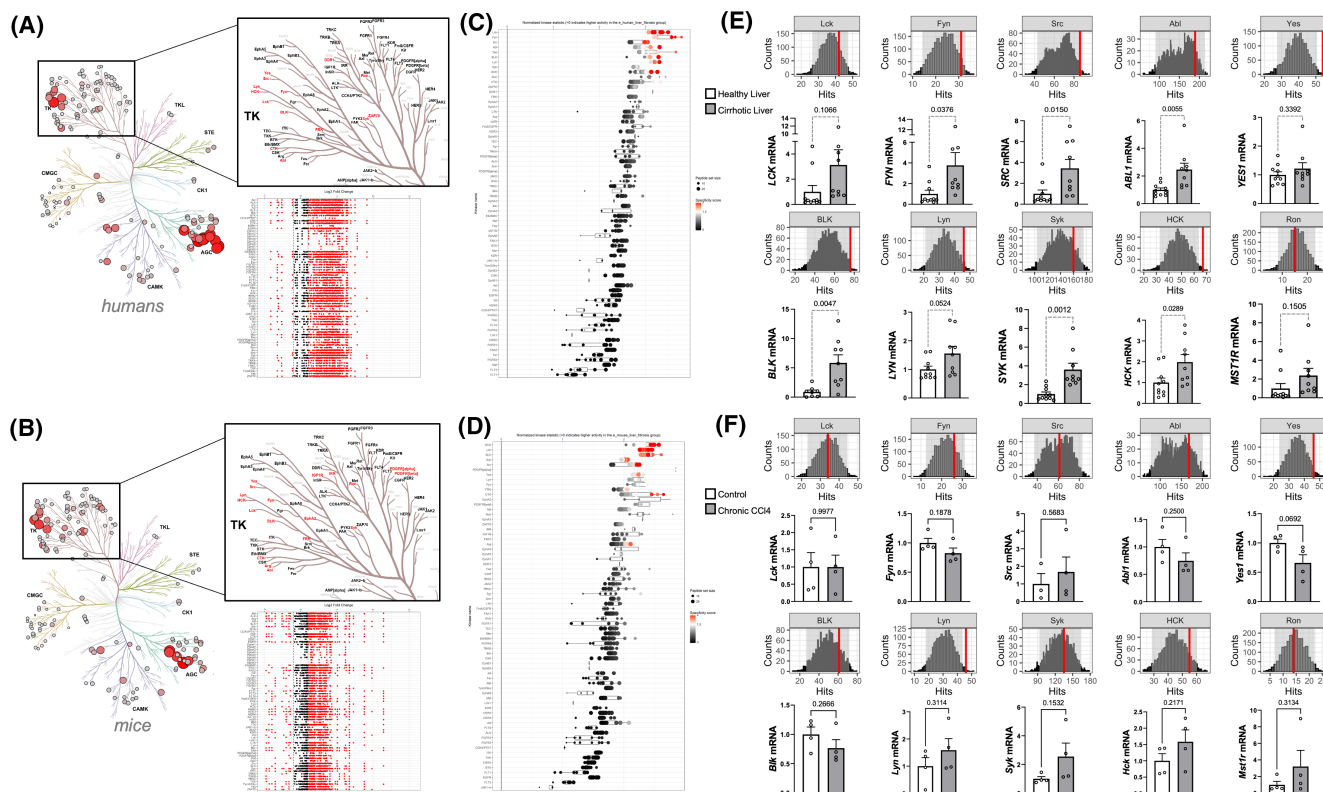


FIGURE 4 Interrogation of individual tyrosine kinases in fibrosis of humans and rodents. Paralogous phylogenetic comparisons of differentially active (red text) tyrosine kinases in human liver fibrosis versus normal control samples (A) or mouse fibrosis versus normal control samples (B). The red dots of the \log_2 fold-change images indicate increased or decreased activity for each individual kinase in fibrosis compared with control. Differentially active individual kinases in human (C) or mouse (D) fibrosis compared with normal samples. Red coloring indicates higher specificity. Quantification of differentially changed individual kinases is shown as histogram peacock plots and mRNA expression measured via real-time PCR in humans (E) or mice (F)

of *DMPK* but not *PRKACA* were higher in humans, with *DMPK* expression being statistically significant. Mice with fibrosis had no statistically significant difference between these two genes. Next, we performed immunostaining using antibodies for *DMPK* (no phospho antibody available), phosphorylation of PKA (pPKA), and α SMA to validate levels and localization of liver cell type. The *DMPK* showed strong expression in the normal healthy human livers and vehicle-treated mice livers (Figure 5E,F). The *DMPK* immunostaining was higher in the cirrhotic human livers but not the CCl_4 -treated mice livers. The *DMPK* was localized outside of the α SMA, indicating that it is likely expressed in hepatocytes. The pPKA had low immunostaining in normal healthy human livers and vehicle-treated mice livers, similar to the pINSR and pDDR1. The staining was higher in the human cirrhotic livers and mice with chronic CCl_4 treatment (Figure 5E,F). The pPKA immunostaining was colocalized with the α SMA in human cirrhotic livers and the chronic CCl_4 -treated mice livers, indicating that this might also be an effect specific to HSCs.

The STK events, unlike the PTK, also had some kinases that had negative Z scores. The kinase families with the most negative Z scores (*DYRK*, *PDK1*, *ERK* [mitogen-activated protein kinase 8 (*MAPK8*)],

JNK [*MAPK1*]) are represented as expression levels (Figure 5G,H), and peacock plot analysis is shown for each in Figure S2. The results in humans show that gene expression for *DYRK1A*, *PDK1*, and *MAPK1* was significantly higher. The gene expression for these four kinases was not significantly different for mice with fibrosis. However, there was a trend to be lower. Further analysis of the subfamily STKs revealed that some pathways were conserved between humans and rodents with fibrosis (Figure 6A,B). Comparing the most changes in the STK category among humans and mice with fibrosis, several kinases in the PK family were significantly enhanced (Figure 6C,D). The AGC group contains PKA, PKG, and PKC STKs, which is one of the highest bubble plot clusters in the paralog phylogenetic tree in Figure 1. The top-ranked STK kinases include protein kinase C alpha (*PRKCA/PKC α*), protein kinase C beta (*PRKCB/PKC β*), protein kinase C delta (*PRKCD/PKC δ*), protein kinase C theta (*PRKCQ/PKC θ*), protein kinase B beta (*PKB β /AKT2*), protein kinase cGMP-dependent 1 (*PRKG1/PKG1*), protein kinase cGMP-dependent 2 (*PRKG2/PKG2*), protein kinase X-linked (*PRKX*), Pim1 and Pim2, which were the most differentially active STKs between humans and rodents (Figure 6E,F).

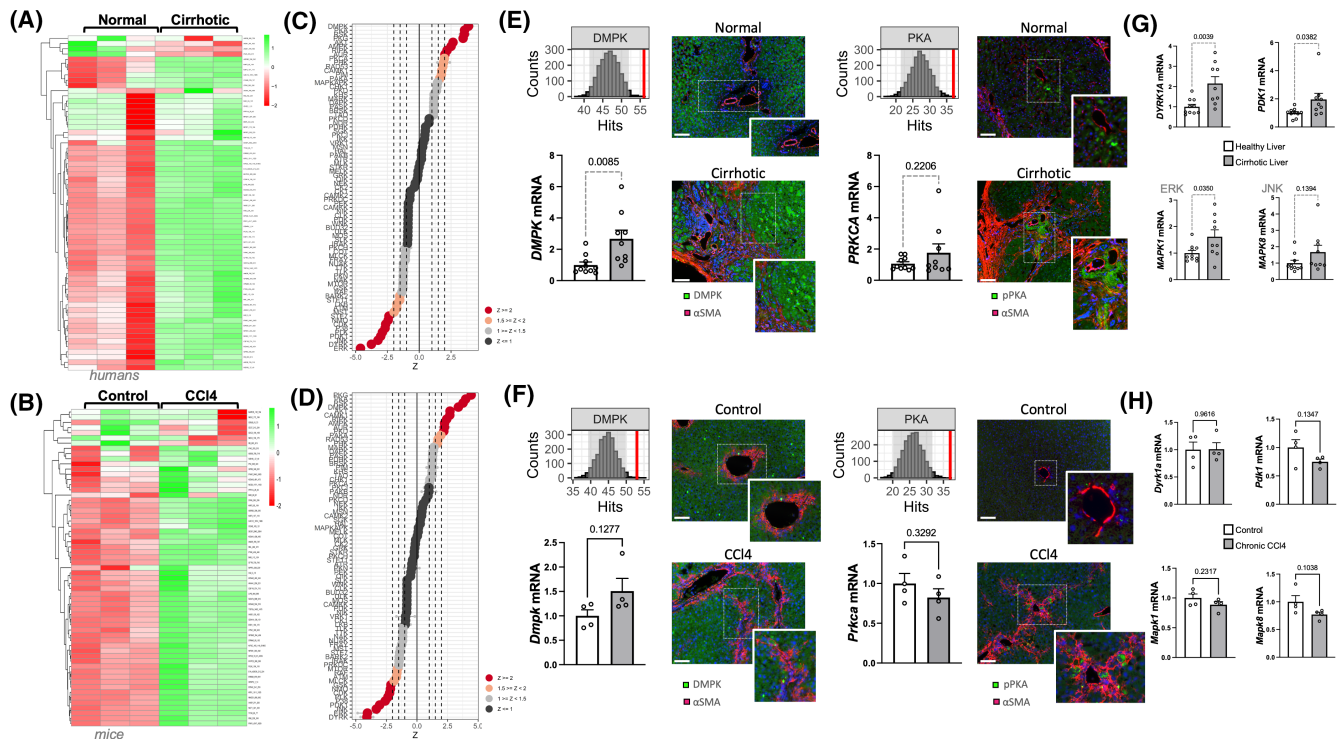


FIGURE 5 Assessment of serine/threonine kinase families changed in fibrosis of humans and rodents. Heatmap of substrate phosphorylation levels for serine/threonine kinases and waterfall plot of serine/threonine family of kinases in humans (A) and mice (B) for fibrotic samples compared with their control. Upstream serine/threonine kinase families identified by peptide substrate phosphorylation in humans (C) or mice (D) fibrotic and normal samples. Quantification of DM1 protein kinase (DMPK) and PKA ($Z > 2$) by histogram peacock plots and mRNA expression measured via real-time PCR and immunostaining with antibodies for DMPK, phospho-PKA (pPKA), or α SMA (scale bar = 50 μ m) in humans (E) and mice (F) for fibrotic samples compared with their control. Real-time PCR measurement of mRNA expression of differentially changed ($Z < 2$) serine/threonine kinases (*DRYK1A*, *PDK1*, mitogen-activated protein kinase 1 [*MAPK1*] [ERK], and *MAPK8* [JNK]) in humans (G) and mice (H)

Comparison of animal models of fatty liver with emerging fibrosis

To validate our findings from the livers of humans with severe fibrosis from cirrhosis and the CCl_4 -induced animal model of fibrosis, we included two additional mouse models that have MAFLD with emerging fibrosis. As we show in Figure 2, we performed sirius red staining in mice fed a choline-deficient (CD) diet compared with chow control or a high-fat plus fructose (HFD+F) diet compared with chow control. As expected, the results show that both of the chow control groups had no fibrosis present (Figure 7A,B). The CD diet had a fibrosis score of 2.0 and a statistically significant induction of *Tgfb1* ($p = 0.0392$) (Figure 7A). The HFD+F diet had a lower fibrosis score of 1.0 and a near (but not significant) induction of *Tgfb1* ($p = 0.0503$) (Figure 7B). These two models are indicative of hepatic steatosis with developing fibrosis, with the CD diet having more developed fibrotic events compared with the HFD+F diet model.

We next wanted to determine whether similar signaling events to the humans with cirrhosis and the CCl_4 -induced fibrosis mouse model were also occurring in these two MAFLD mouse models. The kinome analysis

for the TK substrate phosphorylation levels was compiled into heatmaps for the CD and HFD+F diets and their chow controls. The upstream kinase results were aggregated to form the TK family waterfall plots as described previously. We found that *INSR* was the most differential active kinase in the CD diet compared with chow and that *DDR1* was the third highest (Figure 7C). However, the HFD+F diet compared with the chow-fed group showed that *INSR* and *DDR1* were lower in the livers (Figure 7D). The peacock plots of *DDR1* and *INSR* showed that they had hyperactivity in the CD diet, but both had lower activity in the HFD+F compared with chow diets. The mRNA of *Ddr1* was significantly reduced in the CD diet compared with chow-fed, and *Insr* had no significant difference. For the HFD+F diet compared with chow-fed, neither *Ddr1* nor *Insr* mRNA levels were changed. The STK peptide substrate phosphorylation levels were quantitated for both models and prepared in heatmaps and waterfall plots as described previously. Similar to the humans with cirrhosis and CCl_4 -induced fibrosis models, the CD diet compared with chow control had higher DMPK and PKA kinase activity and no significant differences in *Dmpk* or *Prkaca* mRNA levels (Figure 7E). Interestingly, the HFD+F diet compared with chow control had enhanced

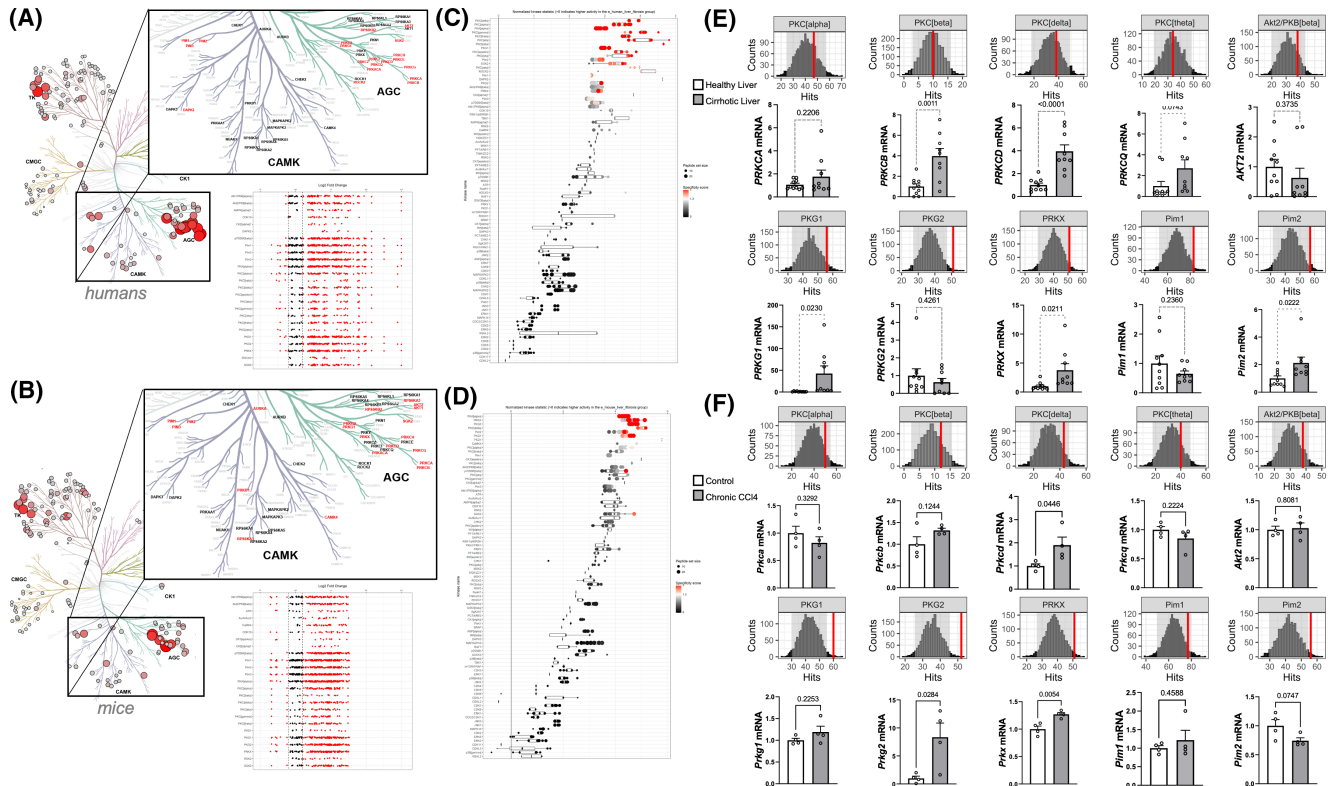


FIGURE 6 Characterization of individual serine/threonine kinases in fibrosis of humans and rodents. Paralogous phylogenetic comparisons of differentially active (red text) protein tyrosine kinase (PTK) in human liver fibrosis samples versus normal control samples (A) or mouse fibrosis versus normal control samples (B). The red dots of the \log_2 fold-change images indicate increased or decreased activity for each individual kinase in fibrosis samples compared with control. Differentially active individual kinases in human (C) or mouse (D) fibrosis samples compared with normal samples. Red coloring indicates higher specificity. Quantification of differentially changed individual kinases is shown as histogram peacock plots and mRNA expression measured via real-time PCR in humans (E) or mice (F)

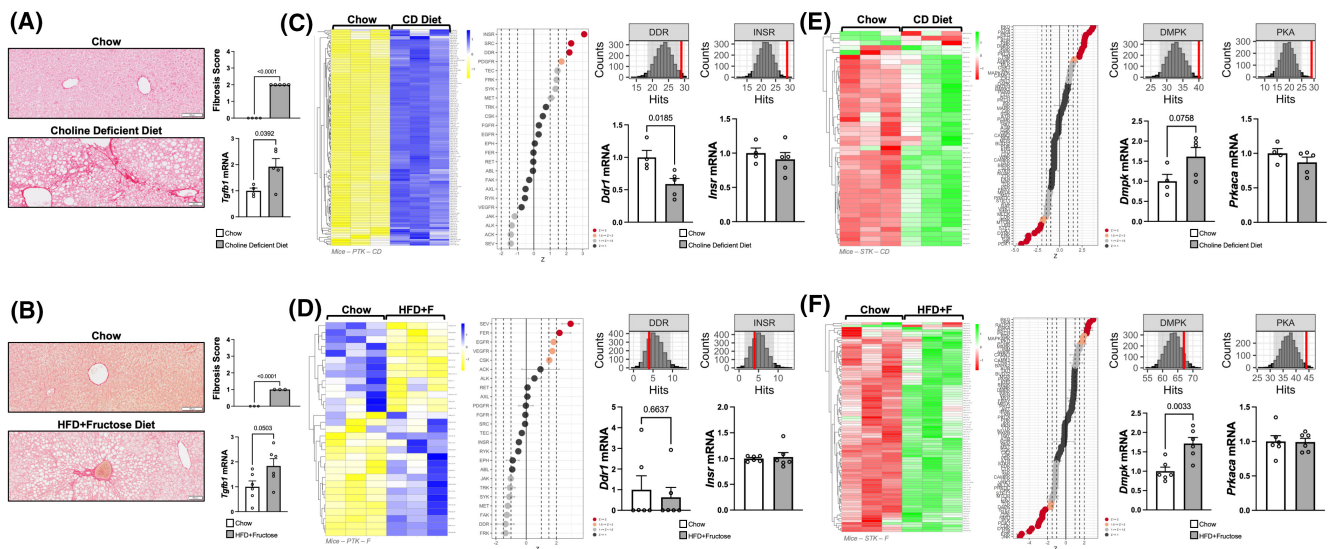


FIGURE 7 Histological and kinomic analysis of additional animal models with fatty liver and emerging fibrosis. Sirius red staining (scale bar = 100 μ m), fibrosis score, and *Tgf- β 1* mRNA expression in the livers of mice fed a choline-deficient (CD) diet and chow control (A) or a high-fat plus fructose (HFD+F) diet and chow control (B). Heatmap of substrate phosphorylation levels for tyrosine kinases, waterfall plot of tyrosine families, peacock plots, and mRNA expression for DDR and INSR in mice fed CD diet and chow control (C) or mice fed HFD+F diet and chow control (D). Heatmap of substrate phosphorylation levels for serine/threonine kinases, waterfall plot, peacock plots, and mRNA expression for DMPK and PKA in mice fed CD diet and chow control (E) or mice fed HFD+F diet and chow control (F)

DMPK and PKA kinase activity (Figure 7E). The *Dmpk* mRNA expression was significantly ($p = 0.0033$) raised in the HFD+F group, and no difference in *Prkaca* mRNA levels.

DISCUSSION

Our studies here ascertained the ability of kinases to phosphorylate a substrate; hence, we measured kinase activity of a complex network of signaling pathways that occur in liver fibrosis (Figure 8), which was compared with the expression level and immunostaining to validate the liver cell type and phosphorylation level. With the help of PamGene PamStation PTK and STK chip array technology, we delineated the critical signaling kinases that were altered in fibrosis of humans and rodents and provided a comprehensive kinase atlas of signaling pathways. The comparisons of these data reveal that the signaling events in humans that cause fibrosis correspond to pathways in rodents with fibrosis. However, these events only corresponded with more advanced fibrosis, such as the finding of pINSR being hyperactive in HSCs of humans with cirrhosis (end-stage fibrosis) with a fibrosis score of 4.0, CCl₄-induced fibrosis in mice that had a fibrosis score of 3.0, and the CD-fed mice with a fibrosis score of 2.0. However, the mice fed a HFD+F diet had a fibrosis score of 1.0 and reduced pINSR activity. The HFD+F model was at the level of developing fibrosis, and this might change with the fibrotic events in the later stages. The vital aspect of this study is that we measured actual kinase activity compared with RNA sequencing of mRNA transcripts, which has no function.

Although perspectives on hepatic fibrosis have grown over the last two decades, this increase in knowledge has yet to produce clinically viable therapies that directly treat hepatic fibrosis.^[1,15,16] The primary obstacle relates to the field's incomplete understanding of the molecular mechanisms and signaling pathways in hepatic fibrosis. Techniques such as high-throughput RNA sequencing can monitor gene-expression levels to reveal interconnected relationships between liver disease and the mRNA levels of kinase pathway genes. Nevertheless, these techniques cannot achieve high-throughput quantification of pathway activity. Our study reveals important relationships between previously published molecular factors such as INSR and DDR1 PTKs and the PK family (PKA, PKB/AKT, PKC, and PKG) of STKs. It is not surprising that the DDR family of transmembrane receptors had increased kinase activity in liver fibrosis, as the ligand for these receptor tyrosine kinases is collagen,^[20] a critical element of the ECM that is shed during HSC proliferation. Although DDR has been investigated within the context of other fibrotic diseases such as in the lungs, pancreas, and kidney,^[2,21,22] its position as a therapeutic target in

hepatic fibrosis is newly emerging. Our results demonstrate increased enzymatic DDR1 kinase activity in fibrosis but do not identify differential enzymatic DDR2 kinase activity in fibrosis for humans or rodents.

The most perplexing finding is that the INSR kinase activity was significantly higher in the liver of humans and rodents with fibrosis. Also, the *INSR* mRNA expression was increased in humans with fibrosis, but the expression was not different in mice. Svegliati-Baroni et al. demonstrated that insulin contributes to the activation of HSCs and stimulates collagen production.^[23] Peterson et al. found that insulin binding was greater in erythrocytes of patients with cirrhosis due to an increase in surface INSR numbers rather than from a change in receptor affinities.^[24] Three independent groups confirmed their findings of higher insulin responsiveness in erythrocytes of patients with cirrhosis.^[25–27] Other studies have shown that humans with cirrhosis have reduced INSR activity in monocytes^[28] and adipocytes,^[29] which might cause the whole body to reduce insulin signaling that could indicate insulin resistance, as measured by glucose intolerance. We found that INSR kinase activity was reduced in mice fed a HFD+F diet. Current research on MAFLD therapeutics is focused on insulin-sensitizers,^[7,8,30] which brings into question whether the latter stages of liver disease (e.g., NASH, fibrosis, cirrhosis) will benefit from insulin-sensitizing drugs. Based on our data from the livers of humans and rodents with fibrosis, there is the possibility that these drugs may exacerbate HSC proliferation, thus worsening liver fibrosis. This concept might be accurate, as it was recently shown by Yen et al. that patients with insulin-resistant type 2 diabetes and liver cirrhosis who used insulin injections were associated with higher risks of death, liver-related complications, cardiovascular events, and hypoglycemia compared to those with the same ailments who did not use insulin.^[31]

We also found that the INSR signaling cascade was significantly increased in mice with CCl₄-induced fibrosis and mice fed a CD diet with higher fibrosis scores that was almost to the level of the human fibrosis, despite sustained mRNA expression of INSR in the animal models. By quantifying kinase activity rather than kinase abundance, we can elucidate ostensible inconsistencies between reports describing insulin receptor functionality in fibrotic contexts as deficient^[32] or impaired.^[33] The increased INSR enzymatic activity detected in our fibrotic samples also relates to the role the AKT kinases play in fibrotic signaling networks. Insulin stimulation of INSR kinase activity leads to downstream signaling events that activate AKT2,^[34] which drives glucose uptake.^[35–38] Enzymatic AKT2 activity was up-regulated in the livers of human and mouse fibrotic samples. Our observation that both INSR and AKT2 enzymatic activities are up-regulated in fibrosis adds weight to the previous hypothesis concerning the mechanism by which insulin signaling contributes to

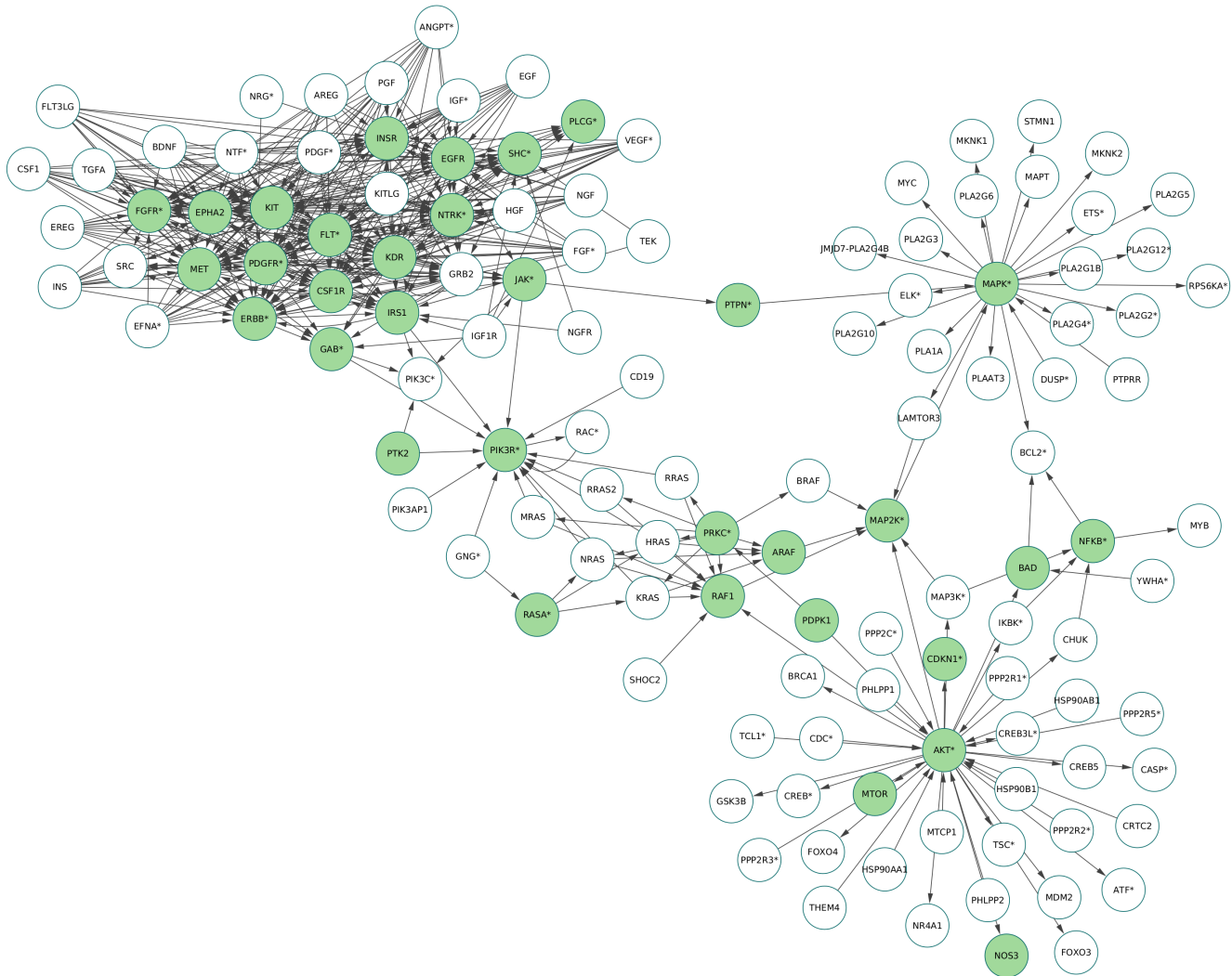


FIGURE 8 Human fibrosis molecular interaction network. Molecular interactions network of human kinomic data to indicate pathways that are changed in fibrosis samples versus control samples. Combined Kyoto Encyclopedia of Genes and Genomes (KEGG) pathways from MAPK, phosphatidylinositol-3-kinase (PI3K), RAS, and EGF receptor (EGFR). Gene nodes were kept if they formed edges with genes in at least three of the four pathways and genes that were noted as differential peptides from humans and mice. Genes from complexes or where multiple genes have very similar symbols were collapsed to single entries, noted with an asterisk (*). Genes from the differential peptides list are green. The network was generated in R using ggraph, visualized in Cytoscape, and laid out using yfiles layouts

fibrosis, that being INSR-mediated PI3K/AKT2 activation of HSCs.^[39,40]

AKT is in the PK class of STKs. Several others in this class were also shown to be significantly higher in kinase activity of humans and rodents with liver fibrosis. DMPK and PKA (represented as *PRKACA*) were the two highest kinase activities changed in fibrosis of humans and mice in the STK family. The *DMPK* gene encodes a protein named the DMPK, which is associated with myotonic DM1 and the degree of metabolic dysfunction in DM1 patients.^[41] *Dmpk* knockout mice have reduced INSR-AKT signaling and develop glucose intolerance.^[42] Bhardwaj et al. suggested that DMPK may have a role in steatohepatitis,^[43] but more studies are needed to clarify its function in fibrosis. One limitation in our study was that there are no phospho-specific DMPK antibodies, which would be useful for showing

where DMPK is most active. Our results here indicated that DMPK might be expressed highest in hepatocytes, as the immunostaining showed very little colocalization with α SMA, a HSC marker.^[19]

Many of the PK family members had hyperkinase activity, as measured by the PamGene technology. The PKA isoform was the most overactive in this group, with PKC and PKG also showing high responsiveness. PKA is a receptor for cAMP and elicits signaling actions that reduce lipid accumulation in the liver.^[44] Hence, antagonizing PKA in the liver leads to hepatic fat accumulation.^[45] In MAFLD, the liver becomes larger due to the accumulation of fat in hepatocytes.^[30] However, in the later stages, such as in the late stage of NASH with fibrosis or cirrhosis, the liver becomes smaller, and lipids are eliminated.^[30] Interestingly, the mice that were fed a HFD+F diet had higher DMPK and PKA kinase activity

compared with chow control, which might indicate that these could be early events that drive some of the fibrotic events that cause progression and worsening of the liver disease. Whether the hyperactive PKA can reduce lipid levels in the latter stages of liver diseases or whether the other PK isoforms may be involved has yet to be explored.

In conclusion, we present a kinomic atlas of hepatic fibrosis that may help resolve potential contradictions in the field while deepening our mechanistic understanding of therapeutically targetable liver fibrosis pathways. The overactive INSR finding was unexpected and may shift the current thinking of the therapeutics for liver fibrosis and cirrhosis in which MAFLD is treated with insulin sensitizers, but this brings into question whether the same treatment might be pernicious for the latter stages of liver dysfunction. This could likely occur from the cell-type rearrangement that happens in the later stages of liver disease, such as hepatocyte death and growth of HSCs. Agents that weaken the fibrotic processes by attenuating HSC activation are promising antifibrotic candidates. Here, the kinome atlas may reflect unknown kinase targets or ones underappreciated that may provide more treatment options. Furthermore, the kinase technology may serve as a better diagnostic tool for determining causes and therapeutics.

ACKNOWLEDGMENTS

The authors thank the Liver Center Tissue Bank at the University of Kansas Medical Center for providing the human liver specimens used in this study. The authors also thank the COVD COBRE Pathology Core at the University of Kentucky for preparing and staining the livers for histology.

CONFLICT OF INTEREST

Dr. Hipp owns employee stocks in Strata Oncology.

AUTHOR CONTRIBUTIONS

Study concept and experiment design: Terry D. Hinds, Jr. *Kinase analysis:* Justin F. Creeden. *Real-time PCR analysis:* Zachary A. Kipp. *Excision of the human livers:* Atta M. Nawabi. *Human liver handling and sample processing and storage:* Steven A. Weinman. *Animal experiments:* Sanjoy Roychowdhury, Samir Softic, Megan R. McMullen, and Laura E. Nagy. *Immunohistochemistry and microscopy analysis:* Mei Xu, Genesee J. Martinez, and Wang-Hsin Lee. *Analysis and scoring of level of fibrosis in the livers:* Jennifer A. Hipp. *Data analysis and interpretation:* Justin F. Creeden, Zachary A. Kipp, Khaled Alganem, Ali S. Imami, Robert M. Flight, Mei Xu, Hunter N. B. Moseley, and S.P. *Extensive bioinformatic analysis of the data and data concordance:* Hunter N. B. Moseley and Robert M. Flight. *Manuscript draft:* Terry D. Hinds, Jr., Mei Xu, Steven A. Weinman, and Justin F. Creeden. *Manuscript review and revisions:* Terry D. Hinds, Jr.,

Justin F. Creeden, Zachary A. Kipp, Mei Xu, Robert M. Flight, Hunter N. B. Moseley, Genesee J. Martinez, Wang-Hsin Lee, Khaled Alganem, Ali S. Imami, Megan R. McMullen, Sanjoy Roychowdhury, Atta M. Nawabi, Jennifer A. Hipp, Samir Softic, Steven A. Weinman, Robert McCullumsmith, and Laura E. Nagy.

DATA AVAILABILITY STATEMENT

Bioinformatic scripts are available on the GitHub repository at the following <https://doi.org/10.5281/zenodo.5714360>.

ORCID

Justin F. Creeden  <https://orcid.org/0000-0003-3123-8401>

Terry D. Hinds Jr.  <https://orcid.org/0000-0002-7599-1529>

REFERENCES

- Roehlen N, Crouchet E, Baumert TF. Liver fibrosis: mechanistic concepts and therapeutic perspectives. *Cells*. 2020;9:875.
- Schuppan D, Ashfaq-Khan M, Yang AT, Kim YO. Liver fibrosis: direct antifibrotic agents and targeted therapies. *Matrix Biol*. 2018;68–69:435–51.
- Lee UE, Friedman SL. Mechanisms of hepatic fibrogenesis. *Best Pract Res Clin Gastroenterol*. 2011;25:195–206.
- Friedman SL. Mechanisms of hepatic fibrogenesis. *Gastroenterology*. 2008;134:1655–69.
- Eslam M, Sanyal AJ, George J, International Consensus P. MAFLD: a consensus-driven proposed nomenclature for metabolic associated fatty liver disease. *Gastroenterology*. 2020;158:1999–2014 e1991.
- Stec DE, Gordon DM, Hipp JA, Hong S, Mitchell ZL, Franco NR, et al. Loss of hepatic PPARalpha promotes inflammation and serum hyperlipidemia in diet-induced obesity. *Am J Physiol Regul Integr Comp Physiol*. 2019;317:R733–R745.
- Hinds TD Jr, Creeden JF, Gordon DM, Stec DE, Donald MC, Stec DE. Bilirubin nanoparticles reduce diet-induced hepatic steatosis, improve fat utilization, and increase plasma beta-hydroxybutyrate. *Front Pharmacol*. 2020;11:594574.
- Stec DE, Hinds TD Jr. Natural product heme oxygenase inducers as treatment for nonalcoholic fatty liver disease. *Int J Mol Sci*. 2020;21:9493.
- Hamoud AR, Weaver L, Stec DE, Hinds TD Jr. Bilirubin in the liver-gut signaling axis. *Trends Endocrinol Metab*. 2018;29:140–50.
- Hinds TD Jr, Hosick PA, Hankins MW, Nestor-Kalinoski A, Stec DE. Mice with hyperbilirubinemia due to Gilbert's Syndrome polymorphism are resistant to hepatic steatosis by decreased serine 73 phosphorylation of PPARalpha. *Am J Physiol Endocrinol Metab*. 2017;312:E244–E252.
- Hinds TD, Sodhi K, Meadows C, Fedorova L, Puri N, Kim DH, et al. Increased HO-1 levels ameliorate fatty liver development through a reduction of heme and recruitment of FGF21. *Obesity (Silver Spring)*. 2014;22:705–12.
- Weaver L, Hamoud AR, Stec DE, Hinds TD Jr. Biliverdin reductase and bilirubin in hepatic disease. *Am J Physiol Gastrointest Liver Physiol*. 2018;314:G668–G676.
- Constandinou C, Henderson N, Iredale JP. Modeling liver fibrosis in rodents. *Methods Mol Med*. 2005;117:237–50.
- Pritchard MT, Nagy LE. Hepatic fibrosis is enhanced and accompanied by robust oval cell activation after chronic carbon tetrachloride administration to Egr-1-deficient mice. *Am J Pathol*. 2010;176:2743–52.

15. Benjamini Y, Hochberg Y. Controlling the false discovery rate: a practical and powerful approach to multiple testing. *J Roy Stat Soc: Ser B (Methodol)*. 1995;57:289–300.
16. Frangogiannis N. Transforming growth factor-beta in tissue fibrosis. *J Exp Med*. 2020;217:e20190103.
17. Cai X, Li Z, Zhang Q, Qu Y, Xu M, Wan X, et al. CXCL6-EGFR-induced Kupffer cells secrete TGF-beta1 promoting hepatic stellate cell activation via the SMAD2/BRD4/C-MYC/EZH2 pathway in liver fibrosis. *J Cell Mol Med*. 2018;22:5050–61.
18. Li H-G, You P-T, Xia YU, Cai YU, Tu Y-J, Wang M-H, et al. Yu Gan long ameliorates hepatic fibrosis by inhibiting PI3K/AKT, Ras/ERK and JAK1/STAT3 signaling pathways in CCl4-induced liver fibrosis rats. *Curr Med Sci*. 2020;40:539–47.
19. Carpino G, Morini S, Ginannicorradini S, Franchitto A, Merli M, Siciliano M, et al. Alpha-SMA expression in hepatic stellate cells and quantitative analysis of hepatic fibrosis in cirrhosis and in recurrent chronic hepatitis after liver transplantation. *Dig Liver Dis*. 2005;37:349–56.
20. Borza CM, Pozzi A. Discoidin domain receptors in disease. *Matrix Biol*. 2014;34:185–92.
21. Moll S, Desmoulière A, Moeller MJ, Pache J-C, Badi L, Arcadu F, et al. DDR1 role in fibrosis and its pharmacological targeting. *Biochim Biophys Acta Mol Cell Res*. 2019;1866:118474.
22. Creeden JF, Alganem K, Imami AS, Henkel ND, Brunicardi FC, Liu S-H, et al. Emerging kinase therapeutic targets in pancreatic ductal adenocarcinoma and pancreatic cancer desmoplasia. *Int J Mol Sci*. 2020;21:8823.
23. Svegliati-Baroni G, Ridolfi F, Di Sario A, Casini A, Marucci L, Gaggiotti G, et al. Insulin and insulin-like growth factor-1 stimulate proliferation and type I collagen accumulation by human hepatic stellate cells: differential effects on signal transduction pathways. *Hepatology*. 1999;29:1743–51.
24. Peterson SW, Angelico M, Masella R, Foster K, Gandin C, Cantafora A. Altered insulin receptor processing and membrane lipid composition in erythrocytes of cirrhotic patients. *Ital J Gastroenterol*. 1992;24:65–71.
25. Okada Y. Increased insulin binding to erythrocytes in chronic liver disease. *Acta Med Okayama*. 1981;35:155–64.
26. Petrides AS, Passlack W, Reinauer H, Stremmel W, Strohmeier G. Insulin binding to erythrocytes in hyperinsulinemic patients with precirrhotic hemochromatosis and cirrhosis. *Klin Wochenschr*. 1987;65:873–8.
27. Teng CS, Ho PW, Yeung RT. Down-regulation of insulin receptors in postnecrotic cirrhosis of liver. *J Clin Endocrinol Metab*. 1982;55:524–30.
28. Greco AV, Bertoli A, Ghirlanda G, Manna R, Altomonte L, Rebuzzi AG. Insulin resistance in liver cirrhosis: decreased insulin binding to circulating monocytes. *Horm Metab Res*. 1980;12:577–81.
29. Harewood MS, Proietto J, Dudley F, Alford FP. Insulin action and cirrhosis: insulin binding and lipogenesis in isolated adipocytes. *Metabolism*. 1982;31:1241–6.
30. Ferguson D, Finck BN. Emerging therapeutic approaches for the treatment of NAFLD and type 2 diabetes mellitus. *Nat Rev Endocrinol*. 2021;17:484–95.
31. Yen FS, Lai JN, Wei JC, Chiu LT, Hsu CC, Hou MC, et al. Is insulin the preferred treatment in persons with type 2 diabetes and liver cirrhosis? *BMC Gastroenterol*. 2021;21:263.
32. Dongiovanni P, Meroni M, Baselli G, Bassani G, Rametta R, Pietrelli A, et al. Insulin resistance promotes Lysyl oxidase like 2 induction and fibrosis accumulation in non-alcoholic fatty liver disease. *Clin Sci (Lond)*. 2017;131:1301–15.
33. Dongiovanni P, Valenti L, Rametta R, Daly AK, Nobili V, Mozzi E, et al. Genetic variants regulating insulin receptor signalling are associated with the severity of liver damage in patients with non-alcoholic fatty liver disease. *Gut*. 2010;59:267–73.
34. Stechschulte LA, Wuescher L, Marino JS, Hill JW, Eng C, Hinds TD Jr. Glucocorticoid receptor beta stimulates Akt1 growth pathway by attenuation of PTEN. *J Biol Chem*. 2014;289:17885–94.
35. Smedlund KB, Sanchez ER, Hinds TD Jr. FKBP51 and the molecular chaperoning of metabolism. *Trends Endocrinol Metab*. 2021;32:862–74.
36. Stec DE, Gordon DM, Nestor-Kalinoski AL, Donald MC, Mitchell ZL, Creeden JF, et al. Biliverdin reductase A (BVRA) knockout in adipocytes induces hypertrophy and reduces mitochondria in white fat of obese mice. *Biomolecules*. 2020;10:387.
37. Hinds TD Jr, Burns KA, Hosick PA, McBeth L, Nestor-Kalinoski A, Drummond HA, et al. Biliverdin reductase A attenuates hepatic steatosis by inhibition of glycogen synthase kinase (GSK) 3beta phosphorylation of serine 73 of peroxisome proliferator-activated receptor (PPAR) alpha. *J Biol Chem*. 2016;291:25179–91.
38. O'Brien L, Hosick PA, John K, Stec DE, Hinds TD Jr. Biliverdin reductase isozymes in metabolism. *Trends Endocrinol Metab*. 2015;26:212–20.
39. Cai CX, Buddha H, Castelino-Prabhu S, Zhang Z, Britton RS, Bacon BR, et al. Activation of insulin-PI3K/Akt-p70S6K pathway in hepatic stellate cells contributes to fibrosis in nonalcoholic steatohepatitis. *Dig Dis Sci*. 2017;62:968–78.
40. Zhang F, Zhang Z, Kong D, Zhang X, Chen LI, Zhu X, et al. Tetramethylpyrazine reduces glucose and insulin-induced activation of hepatic stellate cells by inhibiting insulin receptor-mediated PI3K/AKT and ERK pathways. *Mol Cell Endocrinol*. 2014;382:197–204.
41. Mateus T, Martins F, Nunes A, Herdeiro MT, Rebelo S. Metabolic alterations in myotonic dystrophy type 1 and their correlation with lipin. *Int J Environ Res Public Health*. 2021;18:1794.
42. Llagostera E, Catalucci D, Marti L, Liesa M, Camps M, Ciaraldi TP, et al. Role of myotonic dystrophy protein kinase (DMPK) in glucose homeostasis and muscle insulin action. *PLoS One*. 2007;2:e1134.
43. Bhardwaj RR, Duchini A. Non-alcoholic steatohepatitis in myotonic dystrophy: DMPK gene mutation, insulin resistance and development of steatohepatitis. *Case Rep Gastroenterol*. 2010;4:100–3.
44. Wahlang B, McClain C, Barve S, Gobejishvili L. Role of cAMP and phosphodiesterase signaling in liver health and disease. *Cell Signal*. 2018;49:105–15.
45. Yang J, Zhang X, Yi L, Yang L, Wang WE, Zeng C, et al. Hepatic PKA inhibition accelerates the lipid accumulation in liver. *Nutr Metab (Lond)*. 2019;16:69.

SUPPORTING INFORMATION

Additional supporting information may be found in the online version of the article at the publisher's website.

How to cite this article: Creeden JF, Kipp ZA, Xu M, Flight RM, Moseley HNB, Martinez GJ, et al. Hepatic kinome atlas: An in-depth identification of kinase pathways in liver fibrosis of humans and rodents. *Hepatology*. 2022;76:1376–1388. <https://doi.org/10.1002/hep.32467>